Experimental Analysis of Conditions Based Variations of Characteristics and Parameters of Photovoltaic Modules

A.A. AbdElAziz, K.A. Oliba, Kh.A. AbdEl-hameed, O.A. Selim, R.M. Helal, R.A. Asaad, R. AbdEl-nasser, R. Essam, R. Email, S.H. Tolba, and S.S. Zain
Gradutaion Project team. Electrical Power and Machines Department, Faculty of Engineering, Ain Shams University, Cairo Egypt, kholoud.abdelhakam94@gmail.com
Supervisor: Prof. Dr. Mohamed EL-Shimy Mahmoud Bekhet
Professor of electric energy. Electrical Power and Machines Department, Faculty of Engineering, Ain Shams University, Cairo Egypt, mohamed_bekhet@eng.asu.edu.eg, shimymb@yahoo.com; +201005639589

Abstract–This paper presents an experimental determination of the main and advanced characteristics of photovoltaic (solar-PV) modules as affected by variations in the solar irradiance and temperature. In addition, the effects of connecting modules in series, and in parallel are inspected. The measured main characteristics are the current/voltage (IV), and power/voltage (PV) relations, while the advanced characteristics include the form factor (FF), shunt resistance (Rsh), series resistance (Rs), characteristic resistance (Rch), and efficiency (η). The impacts of the various levels of partial shading on the performance of the modules are also presented. Two identical 10 Wp modules are used in the tests. The sun's energy is simulated using two lighting sources: One 1 kW halogen floodlight and four 100 W incandescent lamps. These light sources offer spectral which is very close to that of the black body radiation; however, they provide a lower color temperature in comparison with the sun. Therefore, they closely match the requirements of the IEC 60904-9 Edition2 and ASTM E927-10 standards of solar simulators. The electrical load is represented using two wound rheostats of 1200Ω, and 500Ω. The temperature is measured by a remote temperature sensor, while the electrical variables are measured using digital multi-meters. For cost reduction, the solar irradiance is estimated based on the linear relation between the short-circuit current, and the solar irradiance. The results are presented within the main text, and summarized in the conclusions section. It is found that the parameters such as Rs, Rsh, Rch, FF, and • are not constant, but they are highly dependent on the variations in the irradiance, and the temperature. The salient conclusion is that the standard equivalent circuit model of solar-PV modules that includes constant parameters needs to be significantly enhanced by considering the variations of the circuit parameters as affected by the variations in the solar irradiance and temperature.

Keywords—Photovoltaics; performance testing; performance characteristics; shading; equivalent circuit.

I. INTRODUCTION

The solar energy is considered the main source of most of the renewable energy forms. For example, the wind energy is due to the temperature differences in the Earth's atmosphere, which is mainly due to the position of the Sun in the sky. Consequently, the direct utilization of the Sun's energy is considered a key factor in the green energy systems [1]. Fig. 1 illustrates various types of energy resources.

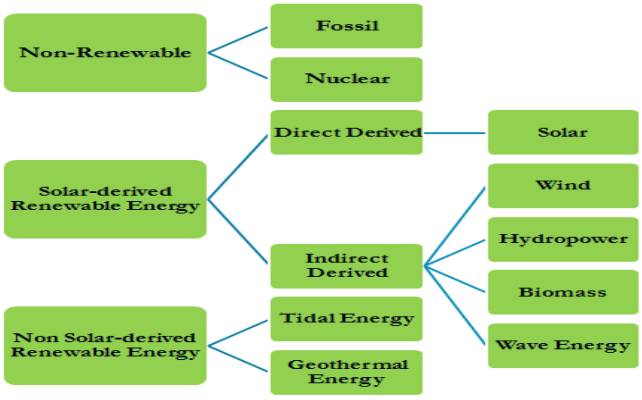

Fig. 1: Energy resources [2]

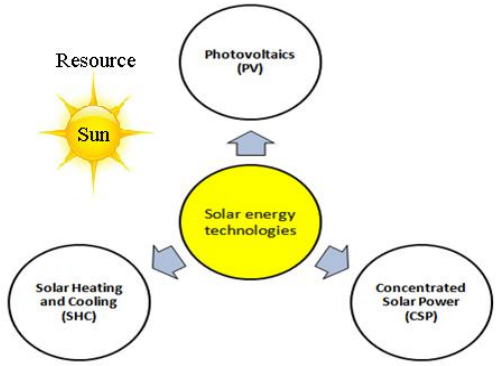

Fig. 2: Basic solar energy technologies [2]

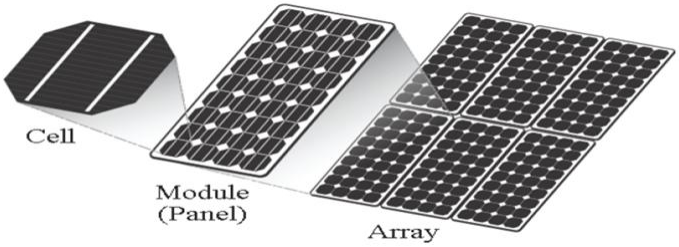

Fig. 3: Solar-PV cell, module (or panel), and array

To be transformed into a desired form, the solar energy technologies (Fig. 2) are constructed by humans for converting the solar energy resource to a desired source of energy. Generally, energy technology is man-made devices, and equipment for converting, transmitting and storing energy

resources. Photovoltaics (solar-PV) are a technology that directly converts the solar radiation to electric energy [2]. Solar-PV technologies has a major advantage over other renewable energy technologies due to their static nature that significantly reduces the required maintenance during their operation, they are also portable, and modular technologies that can fit a wide range of applications starting from μWh energy devices, to GWh energy systems [3]. They also found numerous applications in civil, military, and space systems.

In electric power system applications, solar-PV generators are formed by connecting several solar-PV modules or panels to form a solar-PV array (Fig. 3). The array is connected to suitable DC-DC converters, and DC-AC converters for supplying DC, and AC loads respectively. The converters perform essential functions such as maximum power point extraction, battery charge control, power conditioning (e.g. adjusting the output AC frequency, and voltage magnitude) [1, 2, 4].

II. Characteristics, and Equivalent Circuit

The physical structure of a solar cell is similar to that of the popular P-N junction diode [1, 2].

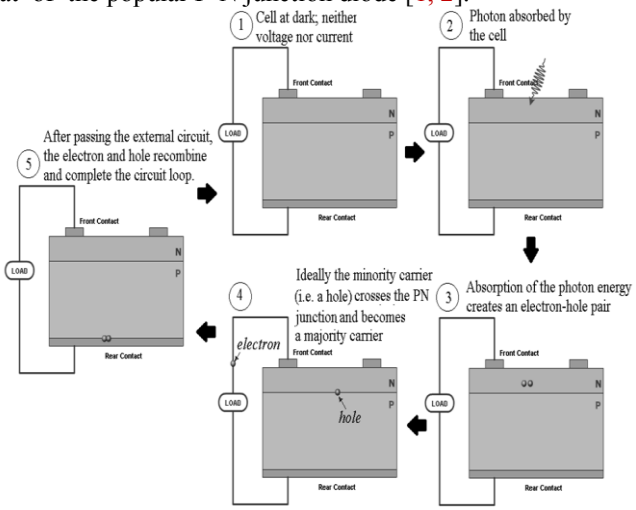

Fig. 4: Concepts of light-generated current [2]

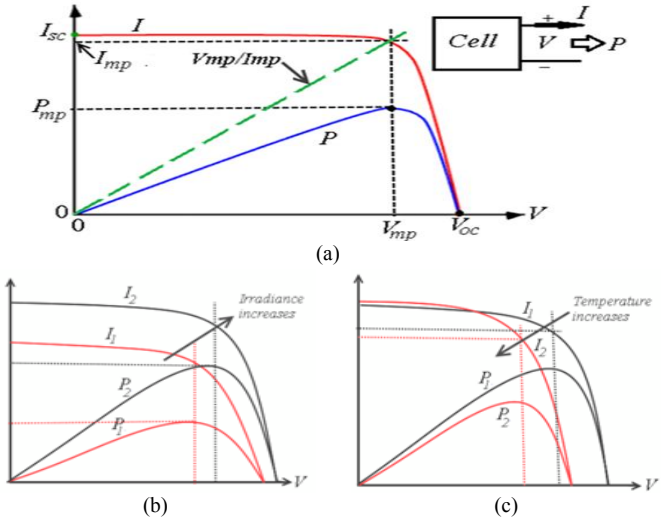

(a) (b) (c)

Fig. 5: Characteristics of solar-PV cells, and impacts of irradiance and temperature variations

When the junction is subjected to sunlight, one of the following conditional situations occurs: (1) If the photon energy is lower than the cell material energy band gap value (which is 1.1 eV for silicon cells), the photons may pass straight through the junction; (2) If the photon energy is higher than the cell material energy band gap value, the material absorbs the photons and generate electron-hole pairs. As a result, an open-circuit voltage appears at the terminals of the junction. This is illustrated in Fig. 4.

Fig. 5 illustrates the basic characteristics of solar-PV cells (i.e. IV, and PV) and the impacts of the changes in the solar irradiance (H) and the cell temperature (T) on the characteristics. It is clear from the figure that the characteristics are dependent on the T and H, but each of the variables has different sensitivity to each of them.

It is shown that the maximum power is directly related to the irradiance, and inversely related to the temperature. The open circuit voltage (Voc) increases with the increase in the irradiance, and it decreases with the increase in the temperature. It shows high sensitivity to the temperature changes in comparison with the irradiance changes. The short circuit current (Isc) significantly increases with the increase in the irradiance, and slightly increases with the increase in the temperature.

The equivalent circuit of a solar cell is shown in Fig. 6 where I_{ph} is the light-generated current which equals to the short-circuit current, and I_D is the diode current (A), I represents the total current which equals to $I_{ph} - I_D$, and V represents the cell terminal voltage.

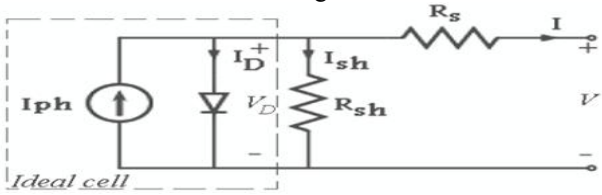

Fig. 6: Equivalent circuit of a solar cell

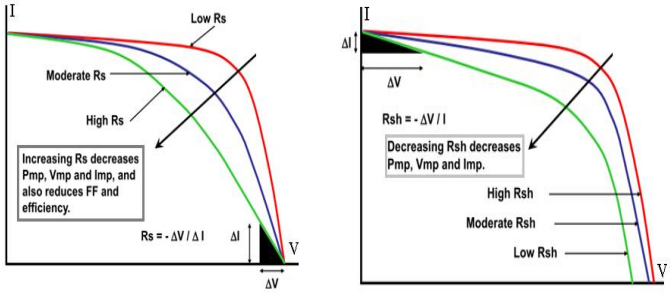

(a) (b)

Fig. 7: Series, and shunt resistances

To account for non-idealities, two resistances are included in the equivalent circuit. The resistivity of the *semiconductor material and the contacts* are represented by a series resistance (Rs) connected at the terminals of an ideal cell. Better representation of the losses can be achieved by adding a shunt resistance (Rsh >> Rs) to represent manufacturing defects in the materials. The impacts of these resistances on the IV characteristics, and their method of estimation are shown in Fig. 7. It is worthy to be mentioned that the values of Rs, and Rsh are considered constant in the mathematical models

describing the IV relations (eq. (1)), while they are not really constant as shown in Fig. 7. This is will also be illustrated later using experimental tests.

$$I = I_{ph} - I_o \left\{\exp\left(\frac{V + IR_s}{V_T}\right) - 1\right\} - \frac{(V + IR_s)}{R_{sh}} \quad (1)$$

Generally, a module having N_{cells} cells connected in parallel and M_{cells} cells connected in series, will then approximately obey the relation shown in equation (2), while an array having N_{mod} modules connected in parallel and M_{mod} modules connected in series, will obey equation (3) [2].

$$\left.\begin{aligned} I_{sc}^{mod} &= N_{cells} I_{sc}^{cell} \\ I_{mp}^{mod} &= N_{cells} I_{mp}^{cell} \\ V_{oc}^{mod} &= M_{cells} V_{oc}^{cell} \\ V_{mp}^{mod} &= M_{cells} V_{mp}^{cell} \end{aligned}\right\} (2) \qquad \left.\begin{aligned} I_{sc}^{array} &= N_{mod} I_{sc}^{mod} \\ I_{mp}^{array} &= N_{mod} I_{mp}^{mod} \\ V_{oc}^{array} &= M_{mod} V_{oc}^{mod} \\ V_{mp}^{array} &= M_{mod} V_{mp}^{mod} \end{aligned}\right\} (3)$$

The *characteristic resistance* (R_{CH}) of a cell, or a module presents an important value as it relates the ideal IV characteristics with the realistic IV characteristics as shown in Fig. 8. The determination of this resistance is also illustrated in the figure.

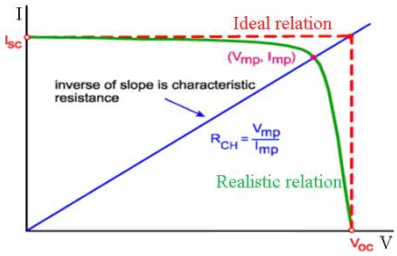

Fig. 8: The characteristic resistance.

Solar-PV cells or modules can be also characterized by some *quality indicators*. These indicators include: (1) The *fill factor* (FF) which ideally equals to unity. In the ideal conditions, the IV relation follows the shape shown in Fig. 8. Practically, the FF is less than unity, and its calculated as,

$$FF = (V_{mp} I_{mp})/(V_{oc}\, I_{sc}) \quad (4)$$

Another important quality indicator is the efficiency (η) is defined as the ratio of electric energy output from the solar cell or module to input energy from the sun. With A being the surface area of the cell, or module, the efficiency is calculated using,

$$\eta = P_{mp}/(G \times A) \quad (5)$$

As previously mentioned and shown in Fig. 3, modules are connected to form an array. A string of series connected modules produces a total terminal voltage equals to the sum of the voltage produced by each of the modules. On the other hand, the current of the string is the same as the current of one module provided that they are identical, and subjected to the same conditions. Parallel connected modules produce a current equals to the sum of the currents produced by all modules, while the terminal voltage is the same as the voltage of one module provided that they are identical, and subjected to the same conditions. If the modules are either non-identical, or subjected to different conditions, the outputs are the averages.

This paper presents a series of experimental tests to study the performance characteristics, and to estimate the quality indicators of a single solar-PV module as well as two identical modules connected in series, and in parallel. In addition, the effects of partial shading are measured. The following sections present the experimental results, and their analyses.

III. Methodology

A. *Components used*

Two identical 10 Wp modules are used in the following tests. The sun's energy is simulated using two lighting sources: One 1 kW halogen floodlight and four 100 W incandescent lamps. These light sources offer spectral which is very close to that of the black body radiation; however, they provide a lower color temperature in comparison with the sun. Therefore, they closely match the requirements of the IEC 60904-9 Edition2 and ASTM E927-10 standards of solar simulators. The electrical load is represented using two wound rheostats of 1200 • , and 500 • . The temperature is measured by a remote temperature sensor, while the electrical variables are measured using digital multi-meters. For cost reduction, the solar irradiance is estimated based on the linear relation between the short-circuit current, and the solar irradiance.

B. *Problems we faced*

Testing has witnessed some different problems. The first issue is the low quality of available solar-PV modules in the market, though they are expensive and rare. This is reflected on their capability to produce the expected outputs. We have to purchase and test many modules in order find appropriate working modules for the use in the tests. Another problem is constructing a low cost light source that mimics the Sun's spectrum, while its temperature production is not too high. We selected to use the mention set of halogen, and incandescent light sources as they produce a good light spectrum [5, 6]; however, they causes a severe increase in the cell temperature when we wanted to increase the illumination to high levels. Therefore, we decided to test the modules at a lower irradiance in comparison with the STC conditions (i.e. 1.0 kW/m^2, and 25^{o}C). We also tested many rheostat resistances and found that the majority of them are unstable i.e. could not change their resistances smoothly. When we tested the shading of half the panel we received unstable measurements. The reason is attributed to the unqualified cheap modules. Initially, we did not consider the time required to keep the panel subject to the light source before measuring the cell temperature. This issue results in erroneous measurements due to the changes in the cell temperature during the tests. By inspecting the temperature rise of the modules, we depicted that 3-5 minutes are sufficient for the cells to reach a steady state temperature which subjected to a light source of a specific intensity. We also used fans to control the cell temperature for performing tests under constant temperature conditions. We also faced a problem with an available inaccurate irradiance meter, and then we decided to apply the linear relation between the maximum power, and the irradiance at constant temperature

for estimating the normal incident irradiance of the module's surface.

IV. Results

A. Impacts of changing the irradiance under constant temperature

In the following tests the temperature is kept around 25°C with ±0.5°C, while changing the irradiance. The results are shown in Fig. 9 to 14. Fig. 9 shows that the previously shown theoretical characteristics of the IV, and PV characteristics are preserved. Fig. 10, and 11 show that all the considered quantities are sensitive to the changes in the irradiance. All of them increases with the increase in the irradiance; however, the sensitivities of the currents, and power are high in comparison with the sensitivities of the voltages, FF, and efficiency.

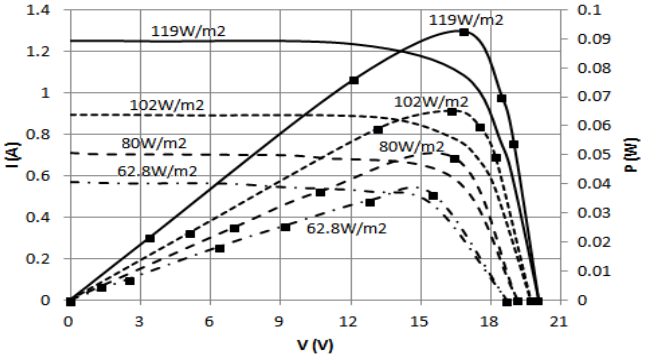

Fig. 9: IV and PV characteristics at different irradiances, and 25°C temp.

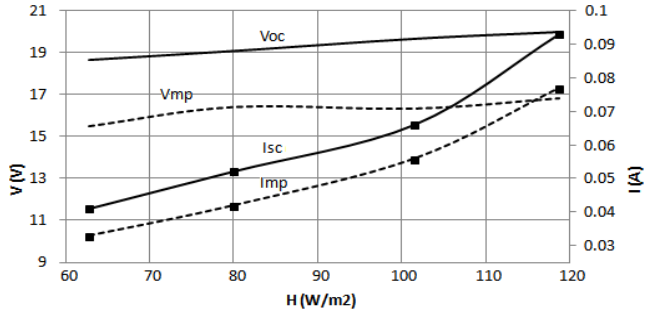

Fig. 10: Variations of Voc, Isc, Vmp, and Imp at different irradiances, and 25°C temp.

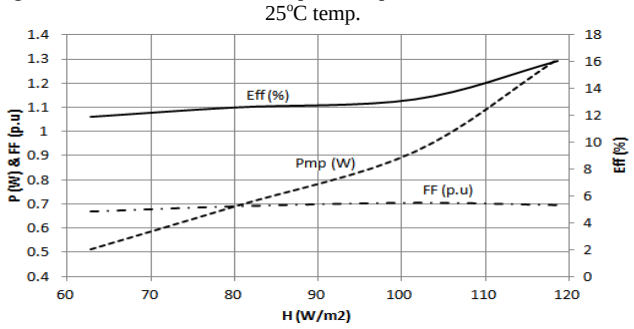

Fig. 11: Variations of the η, Pmp, FF at different irradiances, and 25°C temp.

As expected, the efficiency is increased with the increase in the irradiance at a constant temperature (Fig. 11). The strange changes in the shunt resistance (Fig. 12) are attributed to manufacturing defects, and the nonlinearities of the material impurities. These changes in the FF, and Rs as affected by the changes in the irradiance at constant temperature are shown in Fig. 11, and 12. They are both non-linearly related to the irradiance. It is clear from the results that Rs, and Rsh cannot be considered constant as indicated by equation (1). The changes of the variables, and parameters with the maximum power point are shown in Fig. 13, and 14. These results are useful in the design of the modules as well as the MPPT algorithms. The characteristic resistance shows a linear decrease with the increase in the irradiance (Fig. 12). This is show that matching a resistive load with the module for maximum power extraction, requires a continuous variation of the load resistance to be equal to the characteristic resistance. The series resistance shows a nonlinear decrease with the increase of the irradiance.

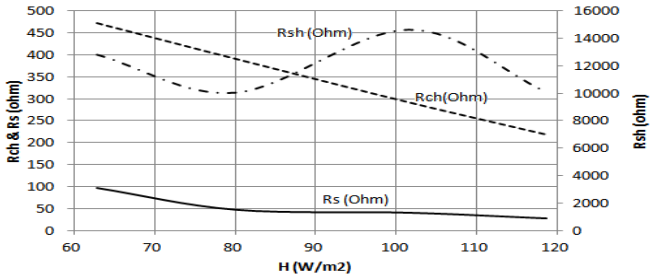

Fig. 12: Variations of Rs, Rch, and Rsh at diff. irradiances, and 25°C temp

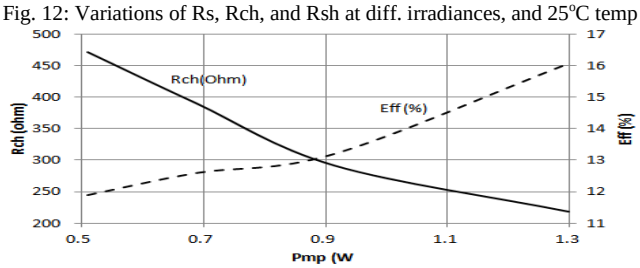

Fig. 13: Variations of Rch, and η with Pmp at constant 25°C temp

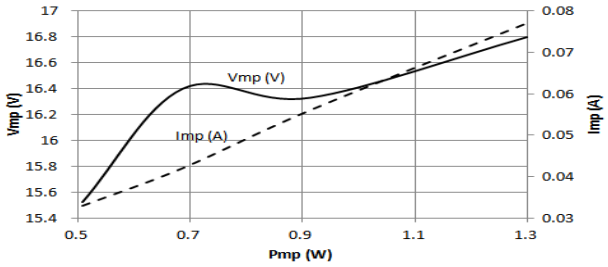

Fig. 14: Variations of Imp, and Vmp with Pmp at constant 25°C temp

B. Impacts of changing the temperature under constant irradiance

In the following tests, the irradiance is kept constant at 154 W/m^2, while the temperature is changed from 25°C to 35°C. The results are shown in Fig. 15 to 20.

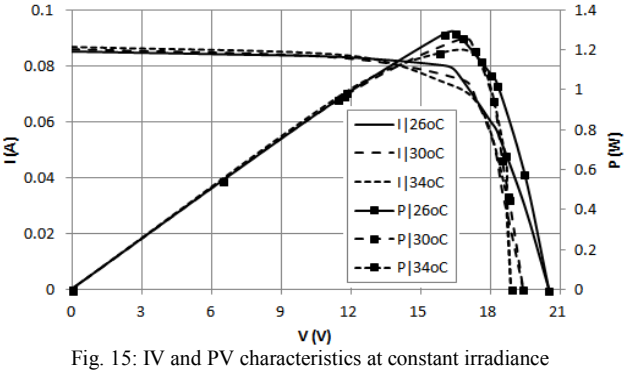

Fig. 15: IV and PV characteristics at constant irradiance

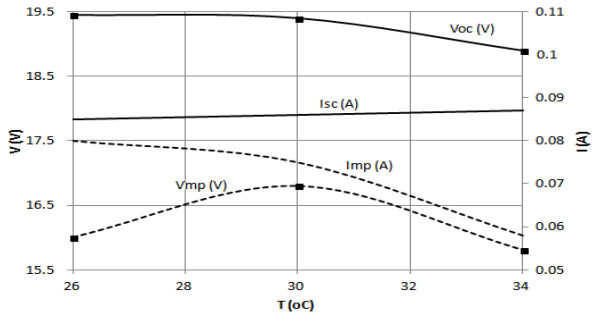

Fig. 16: Variations of Voc, Isc, Vmp, and Imp at constant irradiance

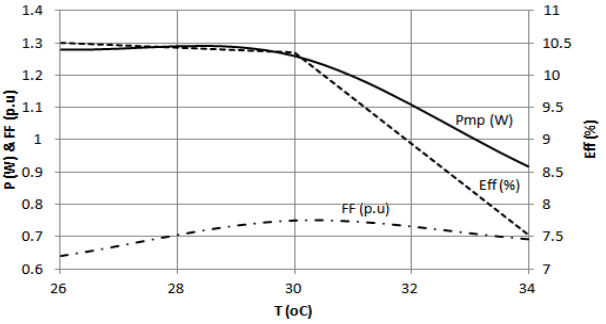

Fig. 17: Variations of the η, Pmp, FF at constant irradiance

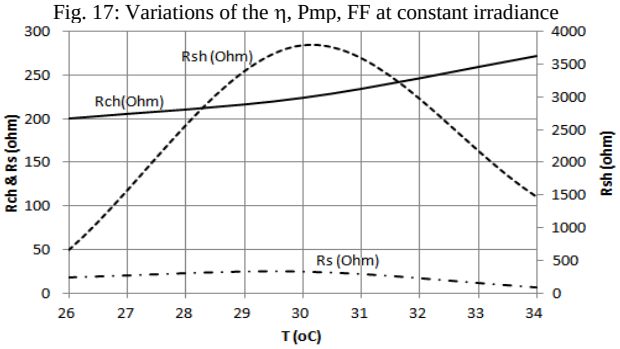

Fig. 18: Variations of Rs, Rch, and Rsh at constant irradiance

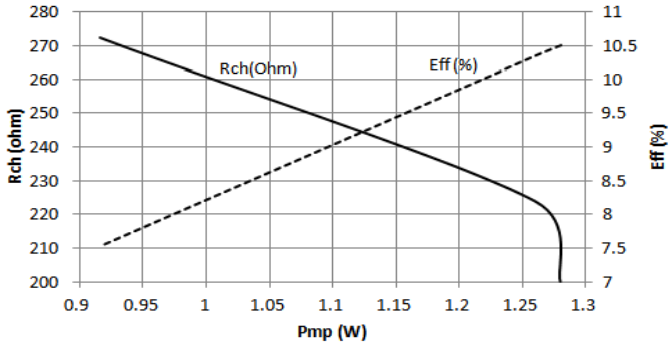

Fig. 19: Variations of Rch, and η with Pmp at constant irradiance

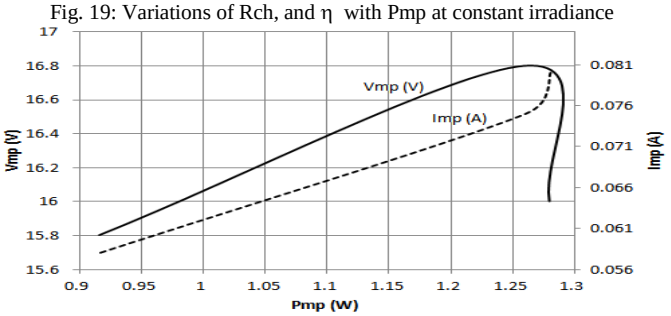

Fig. 20: Variations of Imp, and Vmp with Pmp at constant irradiance

Again, the basic impacts of the changes in the temperature (Fig. 15) are in conformation with the previously described theoretical characteristics. As expected, the efficiency (Fig. 17), and the fill factor (Fig. 18) are nonlinearly decreased with the increase in the temperature. The Isc is slightly increased with the increase of the temperature, while the open circuit voltage decreases with a higher sensitivity. The results also confirm the nonlinear changes of Rs and Rsh with the temperature; however, they show a decreasing trend with the increase in the temperature. The rest of the same results are consistent with the theoretical performances.

C. Characteristics of connected modules at constant temperature

In this section the two modules are connected in series, then in parallel and in each case the performance characteristics are measured at constant temperature. Due to space limits, the basic characteristics (i.e. IV, and PV) are only shown. The results are shown in Fig. 21 to 24.

A comparison between the characteristics of series, and parallel connected modules, easily show the main theoretical conclusions valid. Under the same conditions, the Voc of two modules connected in parallel is half the Voc of the two modules when connected in series. In addition, it is also clear that under the same conditions, Isc of the two modules connected in parallel is nearly double the value of the Isc of the same two modules when connected in series.

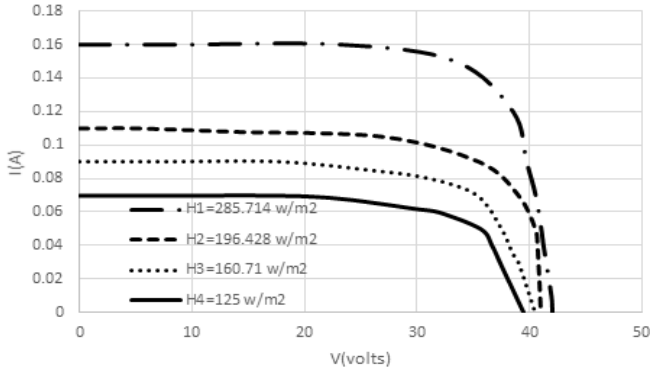

Fig. 21: IV characteristics of a two PV module connected series at different irradiances

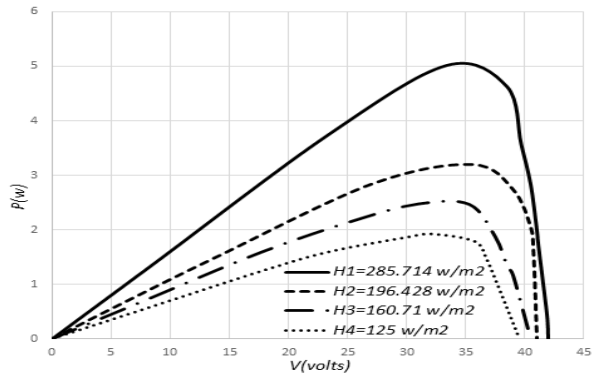

Fig. 22: PV characteristics of a two PV module connected series at different irradiances

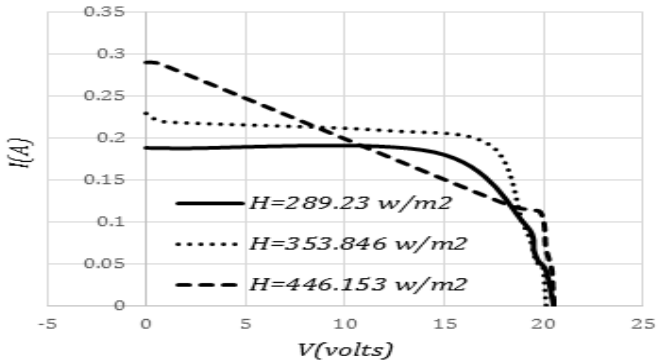

Fig. 23: IV characteristics of a two PV module are parallel connected at different irradiances

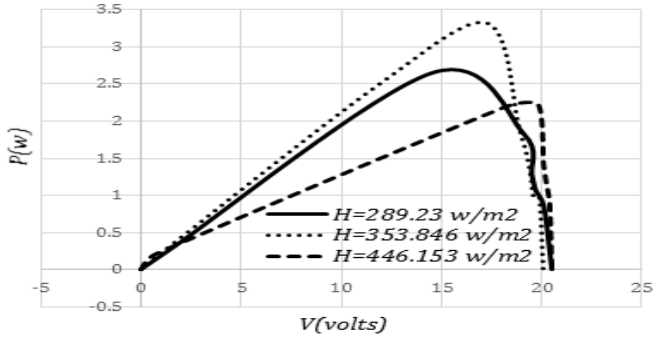

Fig. 24: PV characteristics of a two PV module are parallel connected at different irradiances

D. Characteristics of connected modules at constant irradiance

The characteristics of connected modules operating under constant irradiance are shown in Fig. 25 (for series connection), and Fig. 26 (for parallel connection). The results show conformations with the theoretical concepts.

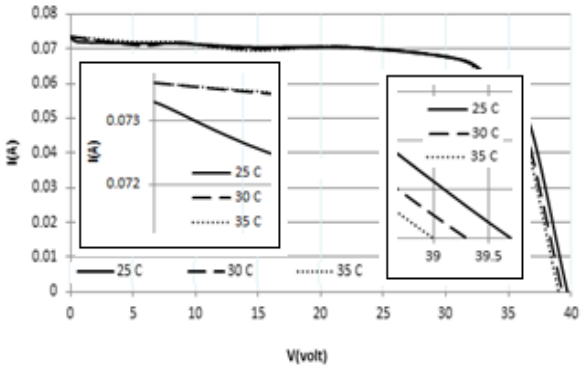

Fig. 25: IV characteristics of 2 series PV modules at different temperature and constant Irradiance

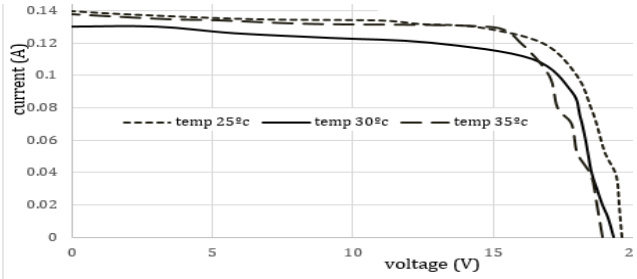

Fig. 26: IV characteristics of 2 PV modules connected in parallel at constant irradiance and different Temperature

E. Characteristics of a single module at various shading levels

The partial shading is a total darkening, or partial reduction of the light intensity incident of a partial area of the module. As a result, non-uniform illumination of the module's surface occurs. In this section total darkening of a partial area of the module is considered. The darkened area is 1/4, or 1/3, or ½ of the module's surface area. The results are shown in Fig. 27, and 28.

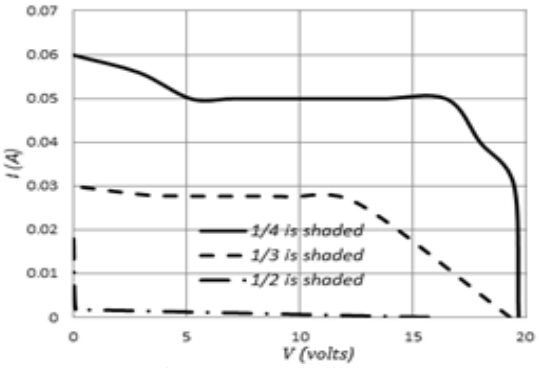

Fig. 27: IV characteristics of a PV module at different shadings and constant temperature

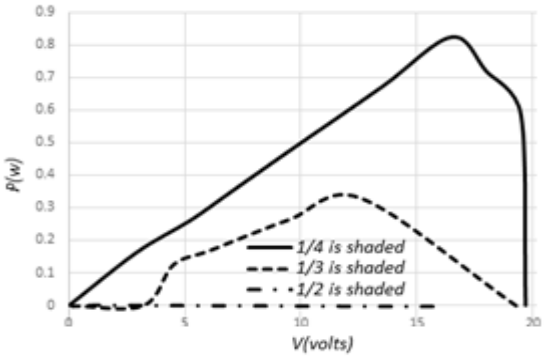

Fig. 28: PV characteristics of a PV module at different shadings and constant temperature

In comparison with Fig. 9, and 10, it is clear that the partial shading highly affects the shape, and the values of the basic characteristics. The severity of the shading is, of course, increase with the increase in the shaded portion of the surface area. These issues are attributed to the intense disturbances in the internal currents, and voltage distribution over the module's incremental areas.

IV. Conclusion

This paper presents a series of experiments for determining the characteristics of solar-PV modules are affected by the irradiance, and temperature as well as the shading, the connection between them. Most of the experimental results match the main theoretical concepts. Since the measurements show high sensitivity of the parameters of the equivalent circuit with the input conditions, it is recommended to modify the equivalent circuit of solar-PV cells or modules for considering the changes of the series, and shunt resistances with the changes in the inputs conditions. The details of the modified equivalent circuit will be

considered as a future work; however, its structure takes the following form,

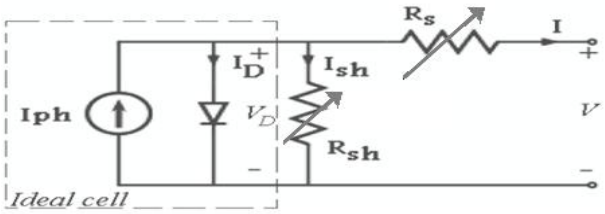

Fig. 29: Modified equivalent circuit

In the modified equivalent circuit, the series and shunt resistances are variable, and they are functions of the temperature, and irradiance. Their changes may be represented by either charts, or supplementary equations for enhancing the capability of the circuit model to closely match the performance characteristics.

REFERENCES

[1] http://pveducation.org/

[2] M. EL-Shimy. Dynamic Security of Interconnected Electric Power Systems - Volume 2: Dynamics and stability of conventional and renewable energy systems. Lambert Academic Publishing / Omniscriptum Gmbh & Company Kg; Germany; ISBN: 978-3-659-80714-5; Nov. 2015.

[3] J. G. Vargas-Hernández, M. EL-Shimy, A. C. Rangel, L. Nađ. Renewable energy in mexico: development and outlook of photovoltaic (PV) energy. ČASOPIS INŽENJERSTVA OKOLIŠA (JOURNAL OF ENVIRONMENTAL ENGINEERING); ISSN 1849-4714 (Print), eISSN 1849-5079 (Online), Vol. 3, No. 2, Dec. 2016, pp. 41-48.

[4] M. EL-Shimy, ed., Economics of Variable Renewable Sources for Electric Power Production, Lambert Academic Publishing / Omniscriptum Gmbh & Company Kg, Germany, ISBN: 978-3-330-08361-5, May, 2017.

[5] https://en.wikipedia.org/wiki/Solar_simulator

[6] M. Tawfik, X. Tonnellier, C. Sansom, "Light source selection for a solar simulator for thermal applications: A review", Renewable and Sustainable Energy Reviews, 2018 Jul 31, No. 90, pp. 802-813.